Published in final edited form as:
Int J Radiat Oncol Biol Phys. 2013 November 15; 87(4): 832–839. doi:10.1016/j.ijrobp.2013.07.017.

Peripheral dose heterogeneity due to the thread effect in total marrow irradiation with helical tomotherapy

Yutaka Takahashi, Ph.D.[1], **Michael R. Verneris, M.D.**[2], **Kathryn Dusenbery, M.D.**[3], **Christopher Wilke, M.D.**[3], **Guy Storme, M.D.**[4], **Daniel J. Weisdorf, M.D.**[5], and **Susanta K Hui, Ph.D.**[1,3]

[1]Masonic Cancer Center, Division of Hematology, Oncology and *Bone Marrow Transplantation*

[2]Department of Pediatrics, Division of Hematology, Oncology and *Bone Marrow Transplantation*

[3]Department of Therapeutic Radiology, University of Minnesota

[4]Department of Radiotherapy, Universitair Ziekenhuis Brussel

[5]Department of Medicine, University of Minnesota

Abstract

Purpose—To report potential dose heterogeneity leading to underdosing at different skeletal sites in total marrow irradiation (TMI) with helical tomotherapy due to the thread effect, and provide possible solutions to reduce this effect.

Methods and Materials—Nine cases were divided into two groups based on patientsize, defined as maximum left-to-right arm distance (mLRD): small mLRD (≤47 cm) and large mLRD (> 47 cm). TMI treatment planning was conducted by varying the pitch and modulation factor while a jaw size (5 cm) was kept fixed. Ripple amplitude, defined as the peak-to-trough dose relative to the average dose due to the thread effect, and the DVH parameters for 9 cases with various mLRD was analyzed in different skeletal regions at off-axis (e.g. bones of the arm, or femur), at the central axis (e.g. vertebrae), and PTV, defined as the entire skeleton plus 1 cm margin.

Results—Average ripple amplitude for a pitch of 0.430, known as one of the magic pitches that reduce thread effect, was 9.2% at 20 cm off-axis. No significant differences in DVH parameters of PTV, vertebrae, or femur were observed between small and large mLRD groups for a pitch of ≤0.287. Conversely, in the bones of the arm, average differences in the volume receiving 95% and 107% dose (V95, and V107, respectively) between large and small mLRD groups were 4.2% (p=0.016), and 16% (p=0.016), respectively. Strong correlations were found between mLRD and ripple amplitude (rs=0.965), mLRD and V95 (rs=−0.742), and mLRD and V107 (rs=0.870) of bones of the arm.

Correspondence author: Susanta K Hui, PhD, huixx019@umn.edu, TEL:612-626-4484, FAX:612-626-7060, Post Address:420 Delaware Street SE, MMC 494, Minneapolis, Minnesota 55455.

Conflict of Interest
None

Conclusions—Thread effect significantly influences DVH parameters in the bones of the arm for large mLRD patients. By implementing a favorable pitch value and adjusting arm position, peripheral dose heterogeneity could be reduced.

Introduction

Total body irradiation (TBI) has been widely utilized as part of the conditioning regimen for hematopoietic cell transplantation. Relapse is a major obstacle to the success of bone marrow transplantation(1–4). Radiation dose escalation studies have shown lower relapse rates for acute and chronic myelogenous leukemia, but increased treatment related mortality(5, 6). The conformal radiation treatment delivered by the helical tomotherapy (HT) was shown to have the potential to enhance the therapeutic ratio (dose to tumor / organs at risk (OARs)(7)). Using this rationale, targeted total body irradiation, referred as to total marrow irradiation (TMI), is becoming an important investigative treatment as a conditioning regimen for hematological malignancies(7–17).

In patients with acute leukemia, it is generally assumed that leukemic cells are distributed throughout the entire skeletal bone marrow. Although it is well known that relapse of leukemia or multiple myeloma from extremities is rare, several groups reported localized relapse of acute lymphoblastic leukemia (ALL) in bone marrow of extremities(18) or the relapse of multiple myeloma from humerus where TBI was used as a part of conditioning regimen(19). On the other hand, chronic skeletal system complications including avascular bone necrosis and clinically evident osteoporosis have been observed after compensator-based intensity-modulated total body irradiation of 12 Gy(20). Homogeneous dose delivery to entire skeletal region including extremities as well as pelvic bone, and vertebrae is therefore essential in TMI treatment planning. Although the dosimetric and physical aspect of TMI with HT are yet to be thoroughly investigated(7, 14, 21–23), the detail dose heterogeneity in different skeletal sites including bones of the arm, vertebrae, and femur has not been reported so far.

HT offers a high intensity modulated beam with multileaf collimator while translating the couch into the gantry(24, 25). This unique feature shows a dose variation pattern that manifests as a ripple which is the results of helical beam junctioning, referred to as the thread effect(26, 27). This characteristic of TMI may lead to heterogeneity of the irradiation dose delivered to the entire skeleton. To our knowledge, no report has been published that investigates the impacts of the thread effects on the dose volume histogram (DVH) in TMI treatment plans in which largely off-axis targets (e.g. bones of the arm such as humerus, radius, and ulna), moderately off-axis targets (e.g. femur) or near central axis targets (e.g. vertebrae) are included. Here we report peripheral dose heterogeneity of TMI treatment delivery, particularly in extremities with HT due to the thread effect.

Materials and Methods

Treatment planning was done with TomoTherapy HiArt Planning Station (Accuray, Inc., Madison, WI). Nine CT datasets were divided into two groups based on patient size, defined as maximum left-to-right arm distance (mLRD): small mLRD (< 47cm) (n=4) and large mLRD (≥47cm) (n=5).

1. Treatment planning

Target and OARs including eyes, lungs, heart, kidneys, liver, brain, and peritoneum were contoured on a Pinnacle treatment planning system (Philips Medical Systems, Palo Alto, CA). Planning target volume (PTV) was generated by adding 1 cm margin to entire

skeletons. To analyze the thread effect at various skeletal sites, we separately contoured bones of the arm including humerus, radius, and ulna, the femur, and the vertebrae.

The prescription of 18 Gy/3 fractions was used for planning simulation to cover PTV with the 85% isodose line. All TMI treatment plans of various pitches of 0.200, 0.287, 0.397, 0.430, 0.556, and 0.754 were conducted with a fixed jaw size (5 cm) to keep treatment time within 40 minutes. The preset modulation factor was also changed from 2.5 to 3.0. Treatment planning for 9 cases was conducted with a pitch of 0.287 and a modulation factor of 2.5 to analyze the differences in DVH parameters between large and small mLRD groups. Furthermore for the five cases in the large mLRD group, a treatment plan with the pitch of 0.200 was also conducted.

For optimization, the same dose constraints for both the PTV and OARs were used for 9 cases.

2. Analysis of the thread effect

We recorded the dose in a slice by slice basis in transverse planes at the identical position of off-axis distances of 0 cm, 10 cm, 15 cm, and 20 cm. These approximately correspond with vertebra, ribs, outer side of femur, and bones of the arm.

Ripple amplitudes due to the thread effect, defined as the peak-to-trough dose relative to the average dose as shown in the formula (1)(26, 27), were calculated at near the central axis, and the off-axis distances of 10 cm, 15 cm, and 20 cm.

$$\text{Ripple amplitude}(\%)=\frac{2(\max(\mathrm{D})-\min(\mathrm{D}))}{\max(D)+\min(D)}\times 100 \quad (1)$$

The correlation between the mLRD and the ripple amplitude was analyzed by Spearman's rank correlation coefficient using Dr. SPSS II software (IBM, New York, NY).

For real time *in vivo* measurement of thread effect, we placed a GafChromic EBT3 film (ISP technologies, Inc, Wayne, NJ) on the forearm during a TMI delivery. The film was scanned by a flatbed scanner (EPSON, Nagano, Japan) as described here(28, 29), and then analyzed by the Dkan2 software (Oras, Osaka, Japan).

3. Plan evaluation

We evaluated the DVH parameters including median dose (D50), the dose received to 5 cc of the volume (D5cc), and the volumes at the dose level of 95% (V95), 107% (V107), and 110% (V110) of the prescription doses in the regions of bones of the arm, vertebrae, femur, and PTV for the 9 cases. All statistics were done using Dr. SPSS II software. The correlations between mLRD and these DVH parameters, and the statistical significances between large and small mLRD groups were evaluated by Spearman's rank correlation coefficient, and Mann-Whitney U test, respectively. For the statistical significance of DVH parameters between pitches of 0.287 and 0.200 of the patients in the large mLRD group, two tailed paired t-test was performed with the null hypothesis that the mean values of DVH parameters in bones of the arm between pitches of 0.200 and 0.287 were not different. Statistical significance was set at a p value of < 0.05.

Results

1. Thread effect analysis

Figure 1 shows the dose distributions and ripple amplitudes in a case (mLRD=47 cm) in a coronal plane at various pitches. Using pitches of ≤0.287 reduced the thread effect at both the vertebrae and bones of the arm (Figures 1 (a), (c)). Dose inhomogeneity at the vertebrae was greater at a pitch of 0.397 than at 0.430 (Figures 1 (e), (g)). On the contrary, peripheral regions (e.g. arm) showed greater dose inhomogeneity due to the thread at a pitch of 0.430 than at 0.397 (Figures 1 (e), (g)). The worst dose inhomogeneity due to the thread effect was found at the pitch of 0.556 (Figure 1 (i)).

The average ripple amplitude was less than 2% at a pitch of 0.200 even at a largely off-axis distance (Figure 1 (b)). On the other hand, a pitch of 0.287 and 0.430 increased the average ripple amplitudes in an off-axis distance-dependent manner. Average ripple amplitudes at the off-axis distance of 20 cm were 2.5% and 9.2% at pitches of 0.287 and 0.430, respectively (Figures 1 (d), (h)). On the contrary, the ripple amplitude at pitches of 0.200, 0.397, and 0.754 did not show off-axis distance dependence (Figures 1 (b), (f), (l)). However, large variations were observed, particularly at the central axis at pitches of 0.397 and 0.754 (Figures 1 (f), (l)). A pitch of 0.556 maximized the ripple amplitude where the maximum value was 25% at an off-axis distance of 20 cm (Figure 1 (j)). The dashed line in Figures 1 (b), (d), (f) and (h) shows the ripple amplitudes at a modulation factor of 3.0. Less than 1% differences in ripple amplitudes were observed between the preset modulation factors of 2.5 and 3.0, of which actual modulation factors were 2.1–2.3, and 2.6, respectively.

The measured dose with GafChromic at an off–axis distance of about 25 cm film also showed the thread effect (Figure 1 (m)).

Ripple amplitude was smaller in the brain, lung, kidney and bladder regions compared to other high-dose regions, including the pelvic and skull bones (Figure 2).

2. DVH analysis

Figures 3 (a), (b), and (c) show the DVHs of the PTV, vertebrae, and bones of the arm in a case in the large mLRD group (mLRD= 47 cm), respectively. The pitches of ≥0.556 exhibited greater hot and cold spots in all skeletal regions. Little differences were observed at pitches of ≤0.430 in the DVH of PTV (Figure 3 (a)). In vertebra, little differences were observed between the pitches of ≤0.287 and 0.430. Dose inhomogeneity was larger at a pitch of 0.397 than of 0.430 (Figure 3 (b)). On the contrary, in bones of the arm, small differences were observed between the pitches of 0.397 and ≤0.287. A pitch of 0.430 led to cold and hot spots (Figure 3 (c)). In a small mLRD case (mLRD= 36 cm), small differences were observed at pitches of ≤0.430 (Figure 3 (d)).

To examine whether a pitch of 0.287 is optimal for any cases regardless of mLRD size, we conducted TMI plans with a pitch of 0.287 and a modulation factor of 2.5 for all nine cases. Table 1 shows a summary of DVH data by the small and large mLRD groups. Significant differences in D5cc, V95, V107, and V110 were observed between the large and small mLRD groups in bones of the arm but not in the PTV and vertebrae. Average V95 of bones of the arm was 99.5% (range, 98.7%–100.0%) and 95.3% (range, 88.2%–98.9%) in small and large mLRD groups, respectively (p=0.016). The corresponding data of V110 were 1.0% (range, 0.3%–1.7%) and 5.0% (range, 2.5% –7.9%), respectively (p=0.016). The largest difference between the large and small mLRD groups was found in V107 of the bones of the arm with an average value of 4.2% (range, 1.6% –5.6%), and 19.7% (range, 15.9% –24.5%), respectively (p=0.016).

Since we found variations in dose heterogeneity in the large mLRD group cases as shown in Table 1, we further examined whether a smaller pitch improves dose heterogeneity in bones of the arm. In a case of an mLRD of 63 cm, a large thread effect was observed even at a pitch of 0.287 (Figure 4 (a)), but this was reduced with a pitch of 0.200 (Figure 4 (b)). The average values of D95, V107 and V110 at a pitch of 0.287 were 95.3% (range, 88.2–99.3%), 21.2% (range, 15.9–26.3%), and 4.9% (range, 2.5–7.9%). The corresponding data at a pitch of 0.200 were 97.2% (range, 88.4–100%), 9.3% (range, 5.5–17.1%), and 0.8% (range, 0.3–2.1%). Statistical significance was observed at D5cc ($p=0.017$), V107 ($p=0.007$), and V110 ($p=0.019$). Although a statistically significant difference in V95 was not observed, V95 was improved by 8% in a case with an mLRD of 63 cm.

3. Correlation analysis between ripple amplitude, mLRD, and DVH parameters

Strong correlation was found between mLRD and ripple amplitude ($rs=0.965$, $p< 0.001$) (Figure 5 (a)). We also found strong correlations between mLRD and D5cc, D50, V95, V107, or V110 with the correlation coefficients of 0.779 ($p=0.013$), 0.866 ($p=0.003$), 0.742 ($p=0.022$), 0.870 ($p=0.002$), and 0.867 ($p=0.002$), respectively (Figures 5 (b), (c), (d), (e), and (f)).

Discussion

We investigated dose heterogeneity at different skeletal regions due to the thread effect in TMI with HT. We found that mLRD strongly correlated with the thread effect and resulted in dose heterogeneity, particularly in bones of the arm. The purpose of TBI is to both assist the immune suppression and to kill malignant hematopoietic cells. In support of this, Endo et al. reported localized relapse of ALL in bone marrow of the extremities (femur and humerus), although relapse from the sternum or iliac bone marrow were also common(18). Bryne et al. reported a relapse of multiple myeloma from the humerus where TBI was used as a part of conditioning regimen(19). In addition, little is known about the biology of hematopoiesis in the extremities. These facts suggest the absolute importance of homogeneous dose delivery even for the extremities.

To minimize the thread effect, we analyzed the pitch and modulation factor that may influence on the DVH parameters according to mLRD. The thread effect is periodic in nature and is caused by various periodic factors including the inverse square law, attenuation, cone effect, and profile divergence. Kissick et al. reported a pitch of 0.86/n (n is integer) minimizes the ripple amplitude(27). More recently, Chen et al. theoretically analyzed the thread effect and found that some optimal pitches are similar to those of Kissick et al. (0.86/n) (27) but are not universal for a larger off-axis distance(26). Although several studies have investigated the optimal pitch for various localized tumor including prostate(30), head and neck(31), and pediatric cranio-spinal irradiation cases(32), these targets are not located at a largely off-axis distance. In TMI treatment planning, the target is located at both near the central axis such as vertebrae and largely off-axis (e.g. bones of the arm). Although several groups have used various pitches from 0.287 to 0.45 for TMI treatment planning(10, 14, 15, 17, 22), these studies did not specifically investigate the DVHs of off-axis targets. Because off-axis target volume is small, the effect is masked under the commonly used large volume of PTV. We found that a pitch of 0.86/2 or even 0.86/3 leads to cold and hot spots in bones of the arm for extremely large mLRD cases (ie; 60 cm) even though little cold and hot spots were observed at the vertebras and PTV. This is in contradiction to previously reported favorable pitch values(27) that focused on target dose homogeneity at mostly centrally located sites that lay on the central axis of the tomotherapy machine. As targets move away from the central axis of the tomotherapy bore, gaps between two consecutive fan beams will increase due to helicity as shown in Figure 4 (c). We also found that a pitch of 0.200 improved dose homogeneity in the arm bones of cases with an

extremely large body width. This is the first report to identify dose heterogeneity in various skeletal regions as well as the entire skeleton (PTV) in TMI treatment planning.

To characterize the optimal pitch at large off-axis targets, we generated treatment plans with various pitches (from 0.159 to 1.0) with 11 targets with 2 cm diameter and 10 cm length located at various off-axis distances of up to 30 cm (Figure 4 (d)). The results revealed that the pitches that provide local maximum or local minimum shifted as off-axis distance increased (Figure 4 (e)). For example, some local minimums at an off-axis distance of 5 cm were 0.287, and 0.430, while those at 25 cm were 0.235, and 0.375. We further found that ripple amplitudes at pitches of 0.397 and 0.754 were smaller than those at 0.86, 0.43, and 0.287, and the same as those at 0.215 and 0.172 at a 20-cm off-axis distance (Figure 4 (f)). The smallest ripple amplitude at an off-axis distance of ≥25 cm was found at a pitch of 0.200 rather than at any pitches of 0.86/n ($n \leq 5$). The use of a smaller n (e.g. ≤6) reduced ripple amplitude but increased treatment planning time (Data not shown) and may potentially increase the treatment time. These data support our DVH results of TMI planning that a pitch of 0.200 is universal, regardless of off-axis distance.

To identify the factor that affected DVH differences in bones of the arm between the large and small mLRD groups, the correlations between these DVH parameters, mLRDs, and average ripple amplitudes were investigated. Our results showed that mLRD strongly correlates with the average ripple amplitude, D50, D5cc, V95, V107 and V110. This fact clearly shows that the DVH variations in bones of the arm between small and large mLRD groups were derived from the thread effect. These data suggest that the arm should be put as close to the body as possible to reduce mLRD at CT simulation.

In the present study, we demonstrated that bones of the arm in the large mLRD group showed significant hot and cold spots. Currently, dose escalation studies in TMI are being performed by several groups(11, 17). In the clinical trial in our clinic, five dose levels of up to 24 Gy/8 fx were defined. The hot as well as cold spots in the arm should therefore be avoided, particularly in dose escalation situations. The lack of appropriate dosimetric knowledge might increase the probability of relapse or other complications. Our findings will therefore be helpful in avoiding these previously reported issues.

We also found that the thread effect was reduced at the brain, lung and kidney. Chen et al. reported that the use of a higher modulation factor reduced the ripple amplitude(26). Since these are high intensity modulated regions, the thread effect would therefore also be reduced in these regions. However, the DVHs in OARs are more likely to be affected by patient anatomy than by thread effect (Data not shown).

In conclusion, thread effect did not significantly influence the DVHs of PTV, vertebrae, and femur but significantly influences that of the bones of the arm for large mLRD patients. A customized pitch should be considered in TMI planning by mLRD. Pitches of 0.200 for large patients and 0.287 for small patients could provide better dose homogeneity. Peripheral dose heterogeneity could be reduced by implementing the favorable pitch value and adjusting arm position to reduce mLRD distance. Although this study was focused on TMI, our findings are also applicable for other treatments including TBI and total skin irradiation.

Acknowledgments

This work was supported by the National Institute of Health grants (1R01CA154491-01) and PHS Cancer Center Support Grant P30 CA77598.

References

1. Anderson JE, Appelbaum FR, Schoch G, et al. Relapse after allogeneic bone marrow transplantation for refractory anemia is increased by shielding lungs and liver during total body irradiation. Biol Blood Marrow Transplant. 2001; 7:163–170. [PubMed: 11302550]
2. Clift RA, Buckner CD, Appelbaum FR, et al. Allogeneic marrow transplantation in patients with chronic myeloid leukemia in the chronic phase: a randomized trial of two irradiation regimens. Blood. 1991; 77:1660–1665. [PubMed: 2015394]
3. Fraser C, Weigel B, Perentesis J, et al. Autologous stem cell transplantation for high-risk Ewing's sarcoma and other pediatric solid tumors. Bone Marrow Transplant. 2005; 37:175–181. [PubMed: 16273111]
4. Reynolds CP, Seeger RC, Black AT, et al. Model system for removing neuroblastoma cells from bone marrow using monoclonal antibodies and magnetic immunobeads. Cancer Res. 1986; 46:5882–5886. [PubMed: 3756928]
5. Clift R, Buckner C, Appelbaum F, et al. Long-term follow-up of a randomized trial of two irradiation regimens for patients receiving allogeneic marrow transplants during first remission of acute myeloid leukemia. Blood. 1998; 92:1455–1456. [PubMed: 9694737]
6. Gilson D, Taylor R. Total body irradiation. Report on a meeting organized by the BIR Oncology Committee, held at The Royal Institute of British Architects, London, 28 November 1996. Br J Radiol. 1997; 70:1201–1203. [PubMed: 9505836]
7. Hui SK, Kapatoes J, Fowler J, et al. Feasibility study of helical tomotherapy for total body or total marrow irradiation. Med Phys. 2005; 32:3214–3224. [PubMed: 16279075]
8. Corvò R, Zeverino M, Vagge S, et al. Helical tomotherapy targeting total bone marrow after total body irradiation for patients with relapsed acute leukemia undergoing an allogeneic stem cell transplant. Radiother Oncol. 2011; 98:382–386. [PubMed: 21339008]
9. Einsele H, Bamberg M, Budach W, et al. A new conditioning regimen involving total marrow irradiation, busulfan and cyclophosphamide followed by autologous PBSCT in patients with advanced multiple myeloma. Bone Marrow Transplant. 2003; 32:593–599. [PubMed: 12953132]
10. Hui SK, Verneris M, Higgins P, et al. Helical tomotherapy targeting total bone marrow-First clinical experience at the University of Minnesota. Acta Oncologica. 2007; 46:250–255. [PubMed: 17453378]
11. Hui S, Verneris M, Froelich J, et al. Multimodality image guided total marrow irradiation and verification of the dose delivered to the lung, PTV, thoracic bone in a patient: a case study. Technol Cancer Res Treat. 2009; 8:23–28. [PubMed: 19166239]
12. Peñagarícano J, Chao M, Van Rhee F, et al. Clinical feasibility of TBI with helical tomotherapy. Bone Marrow Transplant. 2010; 46:929–935. [PubMed: 20935684]
13. Rosenthal J, Wong J, Stein A, et al. Phase 1/2 trial of total marrow and lymph node irradiation to augment reduced-intensity transplantation for advanced hematologic malignancies. Blood. 2011; 117:309–315. [PubMed: 20876852]
14. Schultheiss TE, Wong J, Liu A, et al. Image-guided total marrow and total lymphatic irradiation using helical tomotherapy. Int J Radiat Oncol Biol Phys. 2007; 67:1259–1267. [PubMed: 17336225]
15. Shueng P, Lin S, Chong N, et al. Total marrow irradiation with helical tomotherapy for bone marrow transplantation of multiple myeloma: first experience in Asia. Technol Cancer Res Treat. 2009; 8:29–38. [PubMed: 19166240]
16. Wong J, Liu A, Schultheiss T, et al. Targeted total marrow irradiation using threedimensional image-guided tomographic intensity-modulated radiation therapy: an alternative to standard total body irradiation. Biol Blood Marrow Transplant. 2006; 12:306–315. [PubMed: 16503500]
17. Wong JY, Rosenthal J, Liu A, et al. Image-guided total-marrow irradiation using helical tomotherapy in patients with multiple myeloma and acute leukemia undergoing hematopoietic cell transplantation. Int J Radiat Oncol Biol Phys. 2009; 73:273–279. [PubMed: 18786784]
18. Endo T, Sato N, Koizumi K, et al. Localized relapse in bone marrow of extremities after allogeneic stem cell transplantation for acute lymphoblastic leukemia. American journal of hematology. 2004; 76:279–282. [PubMed: 15224367]

19. Byrne J, Fairbairn J, Davy B, et al. Allogeneic transplantation for multiple myeloma: late relapse may occur as localised lytic lesion/plasmacytoma despite ongoing molecular remission. Bone Marrow Transplant. 2003; 31:157–161. [PubMed: 12621475]
20. Schneider RA, Schultze J, Jensen JM, et al. Long-term outcome after static intensity-modulated total body radiotherapy using compensators stratified by pediatric and adult cohorts. Int J Radiat Oncol Biol Phys. 2008; 70:194–202. [PubMed: 17869024]
21. Han C, Schultheisss TE, Wong JY. Dosimetric study of volumetric modulated arc therapy fields for total marrow irradiation. Radiother Oncol. 2012; 102:315–320. [PubMed: 21724284]
22. Zeverino M, Agostinelli S, Taccini G, et al. Advances in the implementation of helical tomotherapy–based total marrow irradiation with a novel field junction technique. Med Dosim. 2012; 37:314–320. [PubMed: 22326734]
23. Zhuang AH, Liu A, Schultheiss TE, et al. Dosimetric study and verification of total body irradiation using helical tomotherapy and its comparison to extended SSD technique. Med Dosim. 2011; 35:243–249. [PubMed: 19944588]
24. Mackie T. History of tomotherapy. Phys Med Biol. 2006; 51:R427–R453. [PubMed: 16790916]
25. Mackie TR, Holmes T, Swerdloff S, et al. Tomotherapy: a new concept for the delivery of dynamic conformal radiotherapy. Med Phys. 1993; 20:1709–1719. [PubMed: 8309444]
26. Chen M, Chen Y, Chen Q, et al. Theoretical analysis of the thread effect in helical TomoTherapy. Med Phys. 2011; 38:5945–5960. [PubMed: 22047359]
27. Kissick MW, Fenwick J, James JA, et al. The helical tomotherapy thread effect. Med Phys. 2005; 32:1414–1423. [PubMed: 15984692]
28. Akino Y, Koizumi M, Sumida I, et al. Megavoltage Cone Beam Computed Tomography Dose and the Necessity of Reoptimization for Imaging Dose-Integrated Intensity-Modulated Radiotherapy for Prostate Cancer. Int J Radiat Oncol Biol Phys. 2012; 82:1715–1722. [PubMed: 21620584]
29. Mizuno H, Takahashi Y, Tanaka A, et al. Homogeneity of GAFCHROMIC EBT2 film among different lot numbers. J Appl Clin Med Phys. 2012; 13:198–205.
30. Skórska M, Piotrowski T. Optimization of treatment planning parameters used in tomotherapy for prostate cancer patients. Physica Medica. 2013; 29:273–285. [PubMed: 22521735]
31. Moldovan M, Fontenot JD, Gibbons JP, et al. Investigation of pitch and jaw width to decrease delivery time of helical tomotherapy treatments for head and neck cancer. Med Dosim. 2012; 36:397–403. [PubMed: 21377865]
32. Penagaricano JA, Yulong Y, Corry P, et al. Retrospective evaluation of pediatric craniospinal axis irradiation plans with the Hi-ART tomotherapy system. Technol Cancer Res Treat. 2007; 6:355–360. [PubMed: 17668944]

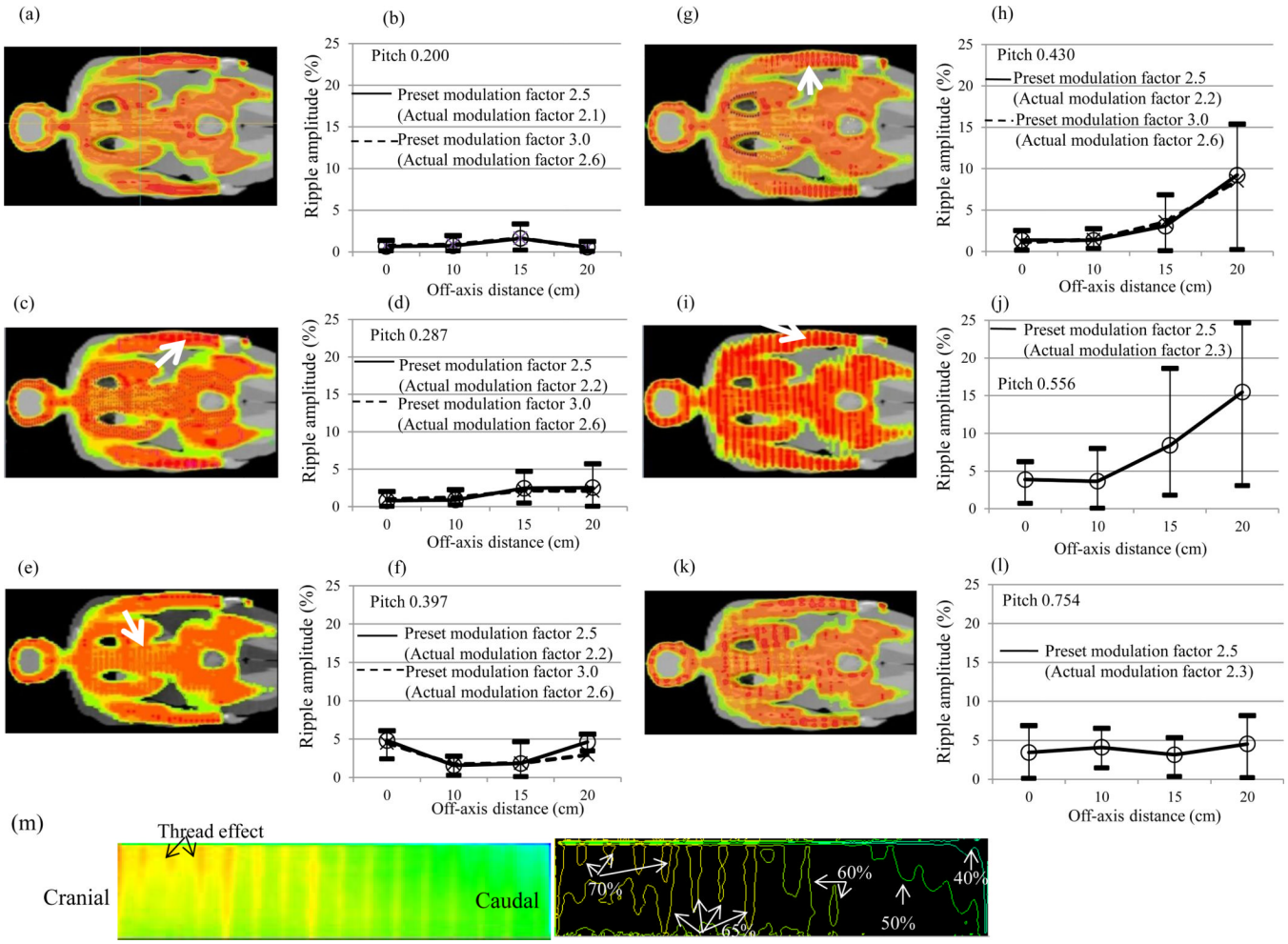

Figure 1.

The dose distributions of TMI planning in a case at pitches of (a) 0.200, (c) 0.287, (e) 0.397, (g) 0.430, (i) 0.556, and (k) 0.754 and the quantitative evaluation of the thread effect with pitches of (b) 0.200, (d), 0.287, (f) 0.397, (h) 0.430, (j) 0.556, and (l) 0.754 with a modulation factor of 2.5 at the central axis and off-axis distances of 10 cm, 15 cm and 20 cm. The upper and lower horizontal bars, and middle circle at each data show the maximum, minimum, and mean ripple amplitudes, respectively. The dashed line shows the corresponding data for a modulation factor of 3.0. (h) Measured dose with GafChromic film on arm region.

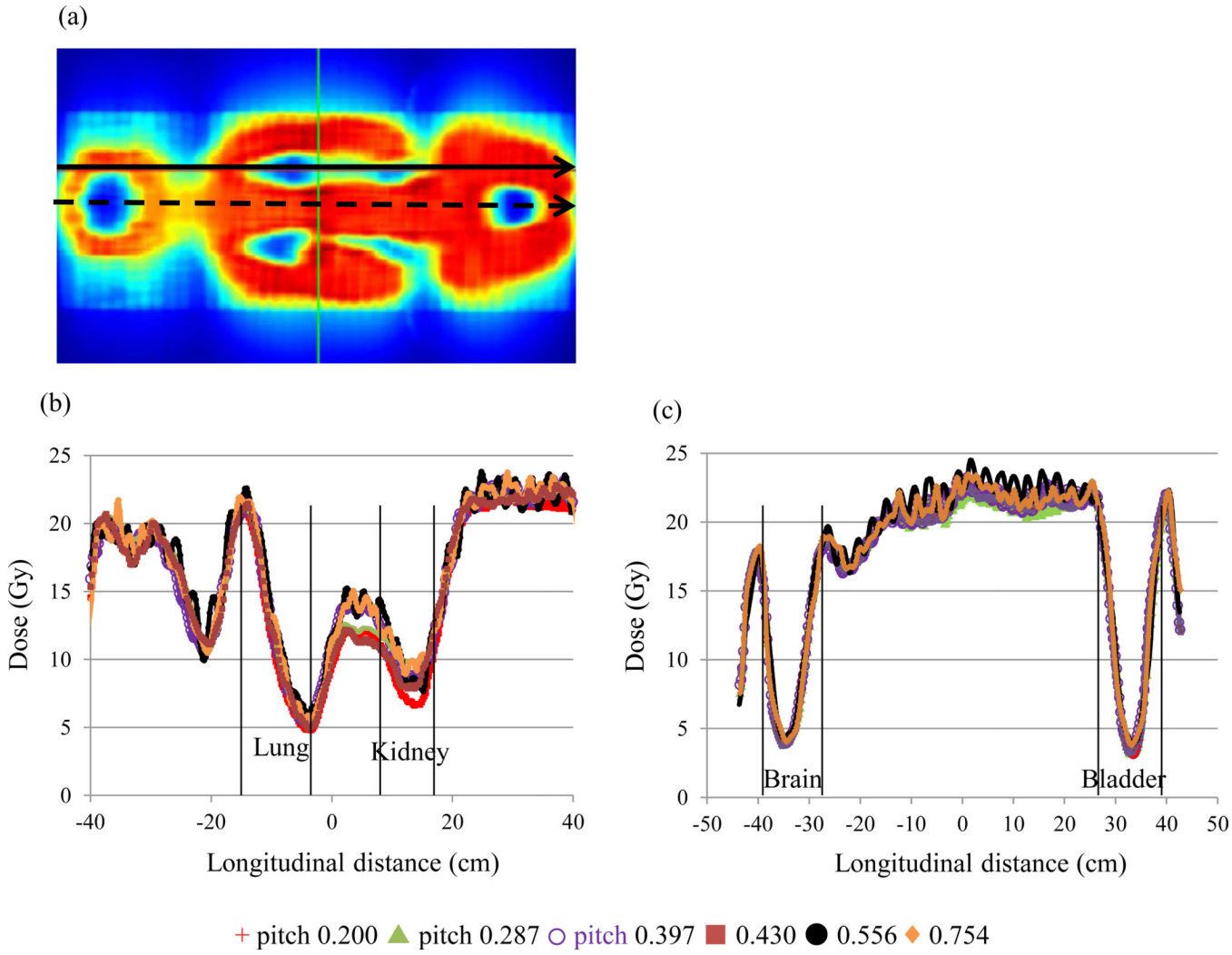

Figure 2.
Thread effects in the brain, lung, kidney, and bladder. (a) Coronal dose distribution in a case, (b) longitudinal profile along the black solid arrow shown in (a), and (c) longitudinal profile along the dashed arrow shown in (a). Small ripple amplitudes were observed in these regions.

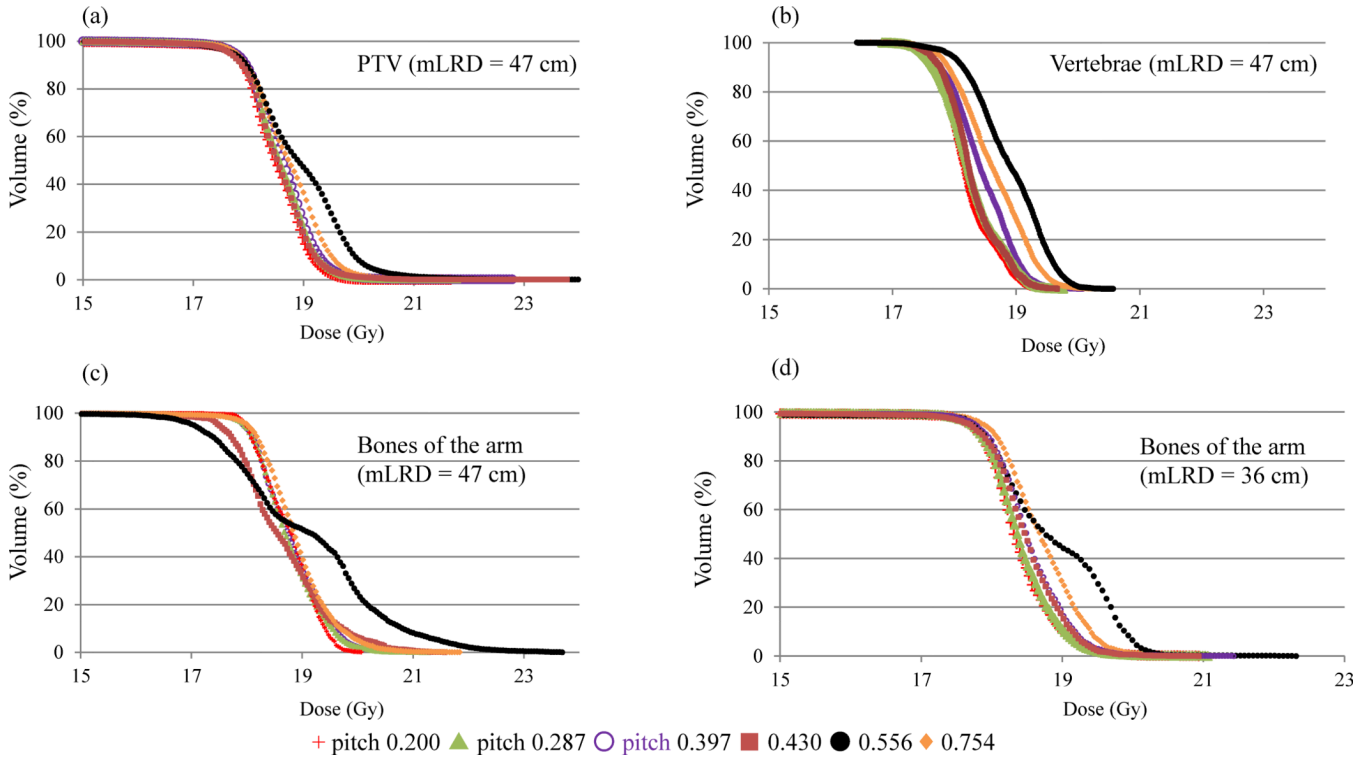

Figure 3.
Dose volume histograms of (a) PTV, (b), vertebrae, (c) bones of the arm from a case in the large mLRD group (mLRD=47 cm) and (d) a case in small mLRD group (mLRD=36 cm).

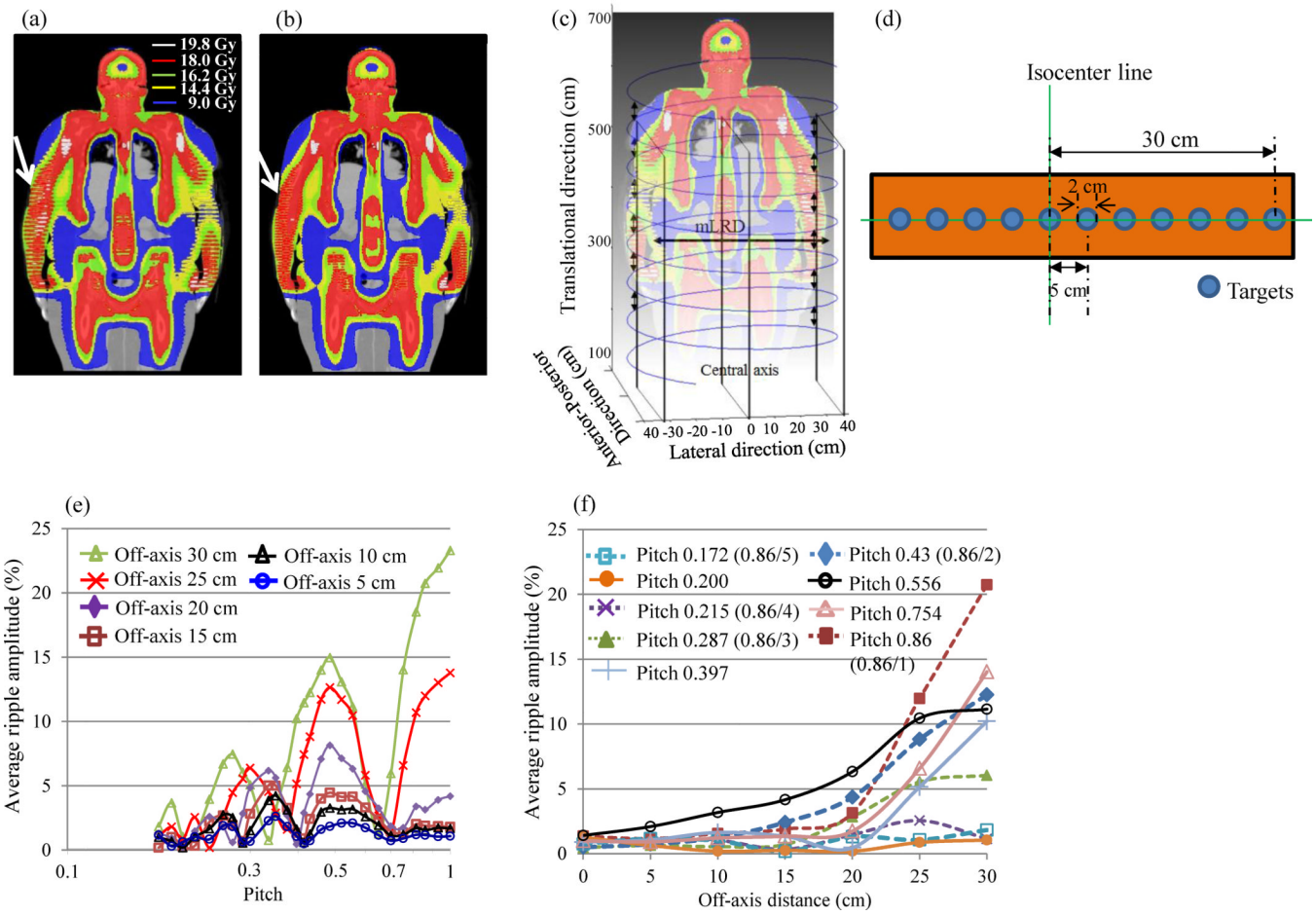

Figure 4.

Coronal dose distribution of an extremely large mLRD patient (mLRD=63 cm) with a pitch of (a) 0.287 and (b) 0.200. Large dose heterogeneity was observed in bones of the arm due to the thread effect at a pitch of 0.287 but was improved using a pitch of 0.200, (c) schema of helical beam junctioning leading to the thread effect, particularly at a large off-axis distance, (d) phantom set up to characterize periodic change in ripple amplitude by pitch, (e) average ripple amplitude by pitch at various off-axis distances, (f) average ripple amplitude by off-axis distance at various pitches.

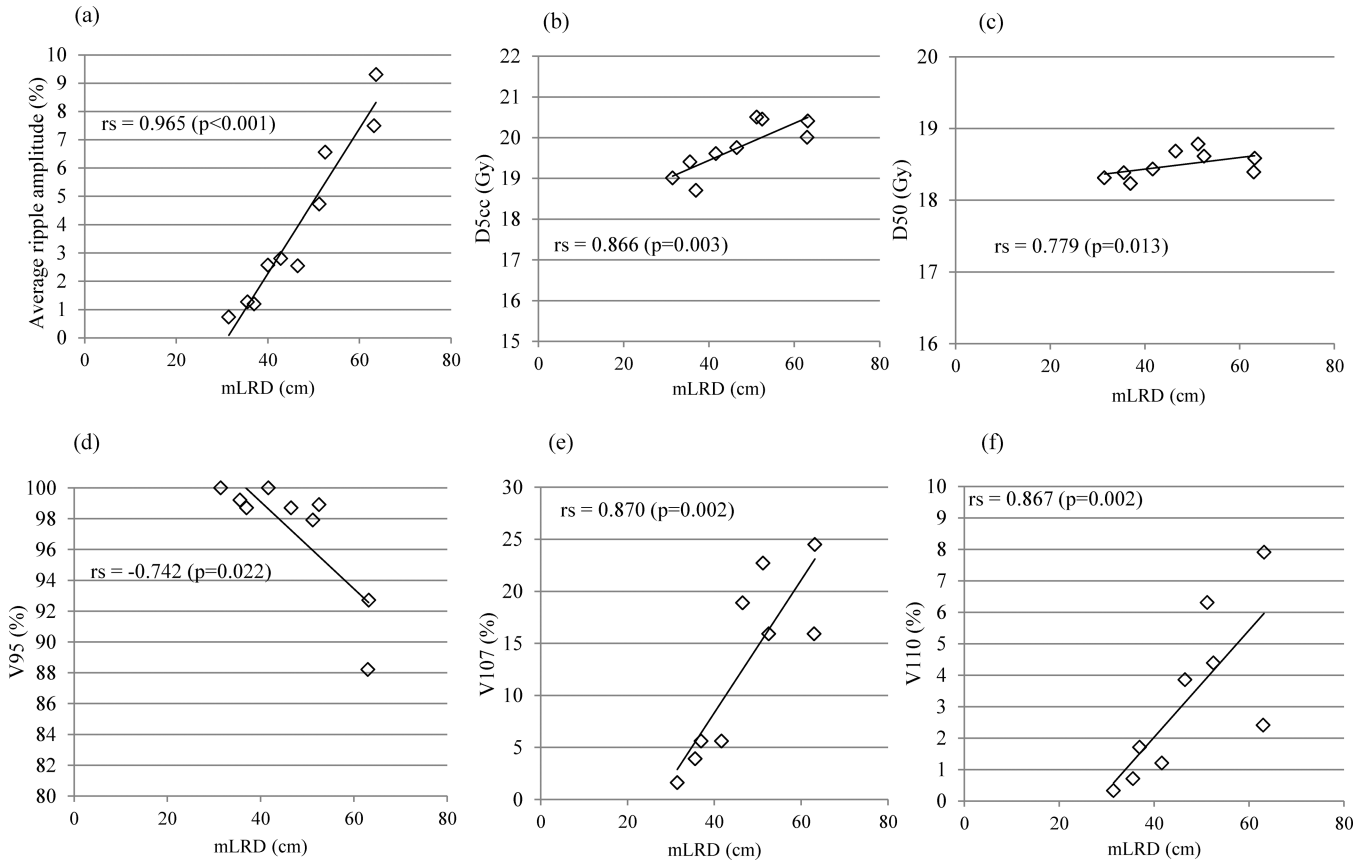

Figure 5.
Correlations between mLRD and (a) average ripple amplitude, (b) D5cc, (c) D50, (d) V95, (e) V107, and (f) V110 at bones of the arm with a pitch of 0.287 for 9 cases.

Table 1

The dosimetric comparison between small and large mLRD groups at different skeletons.

	PTV		Bones of the arm		Vertebrae		Femur	
	Small mLRD	**Large LRD**	**Small mLRD**	**Large LRD**	**Small mLRD**	**Large LRD**	**Small mLRD**	**Large LRD**
D50	18.5 (18.4–18.5)	18.5 (18.5–18.6)	18.3 (18.2–18.4)	18.6 * (18.4–18.8)	18.2 (18.2–18.3)	18.3 (18.2–18.3)	18.3 (18.1–18.4)	18.5 * (18.4–18.7)
D5cc	20.8 (20.1–21.2)	20.5 (19.5–20.9)	19.2 (18.7–19.6)	20.2 † (19.8–20.5)	19.2 (19.0–19.3)	19.4 (19.2–19.6)	19.2 (19.0–19.3)	19.5 * (19.5–19.6)
V95	97.7 (97.6–98.0)	97.4 (96.0–98.7)	99.5 (98.7–100.0)	95.3 * (88.2–98.9)	100.0 (100.0–100.0)	99.9 (99.7–100.0)	98.4 (95.8–100.0)	98.7 (97.0–100.0)
V107	8.0 (7.0–9.1)	7.5 (5.9–9.5)	4.2 (1.6–5.6)	19.7 * (15.9–24.5)	1.2 (0.1–2.1)	1.3 (0.5–2.1)	3.8 (0.8–9.5)	4.3 (0.0–7.9)
V110	1.5 (0.5–2.1)	5.0 (0.8–1.0)	1.0 (0.3–1.7)	5.0 * (2.5–7.9)	0.0 (0.0–0.0)	0.4 (0.0–1.9)	0.0 (0.0–0.0)	0.2 (0.0–1.0)

* p=0.016

† p=0.032

Abbreviations:
mLRD: maximum left-to-right arm distance
PTV: planning target volume